Polymer Chemistry

Accepted Manuscript

ROYAL SOCIETY OF CHEMISTRY

www.rsc.org/polymers

Journal Name RSCPublishing

ARTICLE

Cite this: DOI: 10.1039/x0xx00000x

Received 00th January 2012,
Accepted 00th January 2012

DOI: 10.1039/x0xx00000x

www.rsc.org/

Simulation of radical polymerization of methyl methacrylate at room temperature using a tertiary amine/BPO initiating system

Alexander Zoller, Didier Gigmes, Yohann Guillaneuf*

The decomposition kinetics of the initiation reaction between benzoyl peroxide (BPO) and a tertiary amine, either dimethyl-*p*-toluidine (DMT) or dihydroxyethyl-*p*-toluidine (DHEPT), had been studied by infrared spectroscopy (IR) and an Arrhenius plot had been established. Based on these results a polymerization model of methyl methacrylate (MMA) at room temperature was developed. The model uses both, free-volume models and empirical models for propagation, termination and several side reactions. It describes the conversion in a very broad range of reaction conditions, which are in good agreement with experimental data. This study shows significant differences between DMT and DHEPT in gel time and molar mass of PMMA, which are investigated and explained.

Introduction

Over the last years, an increasing interest in polymerization of MMA and/or other acrylic monomers at room temperature arose for different application fields such as construction,[1] bone surgery,[2, 3] medicinal applications,[4, 5] dentistry[6] and composite.[7-9] The use in dentistry or bone surgery for example needs to be carried out in the human body that means that the polymerization has to be performed at 37 °C.[10] Another challenge is the production of large construction pieces of PMMA such as hulls which can not be heated completely.[11] For these new production opportunities, the polymerization at low temperature is economically and ecologically very interesting as it is an energy saving method without additional heating. A mixture of PMMA and MMA is often used since this syrup enables faster polymerization and higher viscosities, which is easier to handle when manipulated (e.g. dental application). Another advantage of the polymerization of MMA at room temperature is to enable controlling the exothermic reaction inherent to the polymerization of this monomer.

The initiating system composed of benzoyl peroxide in combination with a tertiary amine, such as dimethyl-*p*-toluidine (DMT) or dihydroxyetyhl-*p*-toluidine (DHEPT) for radical polymerization of methyl methacrylate (MMA) at room temperature is known since the 1950s.[12, 13] The mechanism is a complex reaction sequence with a nucleophilic attack of the tertiary amine on the peroxide bond of the BPO molecule followed by a redox reaction and formation of a benzoyloxy radical and a carbon-centered radical derived from the tertiary amine. The kinetics of such reaction has been scarcely studied with only paper about the half-life time obtained by iodometric titration.[12] Based only on polymerization conversion profiles, it was found that the *para*-substituent of the tertiary amine plays an important role on the decomposition kinetics.[13] Basically, an electron acceptor accelerates the reaction and a donor slows it down.

During the bulk polymerization of vinyl monomers and specially the polymerization of methacrylate derivatives, the diffusion of various chemical species plays an important role and many kinetic parameters become quickly diffusion controlled leading to drastic changes of the polymerization rate. Many models were then developed to simulate such systems[14-16] but the room temperature polymerization of MMA was not investigated. Some authors tried to rationalize the kinetics of the bulk polymerization at room temperature of di-functional methacrylate derivatives using numerical simulations.[17] Nevertheless the creation of a solid network requires taking into account several side reactions that could be eliminated in a mono-functional system.

Based on already existing methodologies, this work aims at establishing a robust kinetic model of the radical polymerization at room temperature of methyl methacrylate, using the simulation software PREDICI. This software based on the Galerkin h-p-method and developed by M. Wulkow was proven to be an invaluable tool for describing molecular weight distributions and polymer reaction kinetics for a large range of polymer processes.[18] Compared to other numerical simulations, the model we used required a reduced number of estimated parameters, which are physically meaningful. For the initiation step, which is essential for polymerization reactions, the decomposition kinetics of BPO/tertiary amine was measured by IR and an Arrhenius plot was established, as no kinetic rate constant for the BPO/tertiary amine was described in the literature. For the propagation step, we used the free-volume model developed by Achilias et al.[17] and for the termination model, we adapted an empirical model by Russell et al.[19] The importance of the transfer to the initiator has been also highlighted. Another aspect, which will be discussed in this study is the appearance and the modeling of a bimodal distribution, which has been already observed in the bulk polymerization of MMA at temperatures between 50 and 90 °C.[20] The model was then applied to both, pure MMA polymerization and PMMA/MMA syrup polymerization.

Model development

The different polymerization steps, which were taking into account to model the MMA polymerization initiated by a decomposition reaction involving BPO and a tertiary amine, are shown in Figure 1. After the decomposition step, the anilinomethyl radical and the benzoyloxy radicals initiate the polymerization. We considered that the termination occurs by both combination and disproportionation, even if it is well-known that in the case of MMA, the disproportionation is predominant. [22, 23]

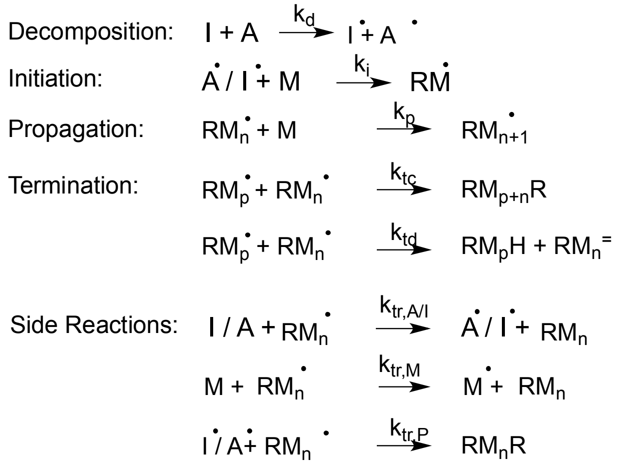

Figure 1. Scheme of a "bicomponent" Free Radical Polymerization (FRP) with I=Initiator, A=Amine, R=Decomposition Component, M=Monomer, radicals are denoted with a dot. f is the initiator efficiency. k_d, k_i and k_p, are respectively the rate constant of decomposition, initiation and propagation. k_{tc} and k_{td} are the rate constant of termination respectively by combination and disproportionation. $k_{tr,A/I}$; $k_{tr,M}$ and $k_{tr,p}$ are the rate constant of transfer respectively to A/I, the monomer and the polymer.

The efficiency of the initiating system is very important to model polymerization reactions. Achilias and coworkers proposed a model for the initiator efficiency and the propagation rate constant which is based on the free volume theory.[17, 24] The term $4\pi N_A r_p D_m$, which is used in the model was taken from the Smoluchowski equation[25] with the Avogadro constant N_A, the effective reaction radius of the polymer r_p and the diffusion coefficient D_m of the monomer. The latter coefficient was usually fitted from polymerization rate and conversion. To estimate such parameter, we used the Achilias equation (see ESI for details) and the experimental data that was experimentally observed by Karlsson and coworkers.[26] This approach led to a good agreement between theoretical and experimental data as shown in Figure 2.

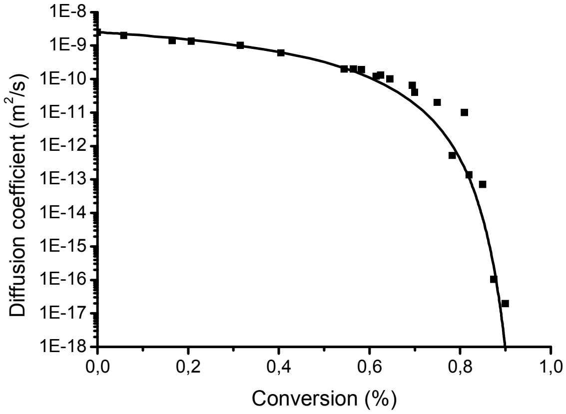

Figure 2. Experimental diffusion coefficient D_m (squares) of MMA in bulk MMA polymerization at 50 °C extracted from reference [26] vs. modeled diffusion coefficient (line).

The termination rate constant k_t is described by mainly four different regions during the polymerization of MMA.[27] The first region is dominated by segmental diffusion where k_t stays almost constant. In the second region the termination rate decreases rapidly as the viscosity increases during the gel effect. The third region has a constant low termination rate where the motion of the polymer becomes very slow and the movement is due to monomer addition at the chain ends. In the last region, k_t declines sharply again due to the glass effect. The IUPAC working group "Modeling of Polymerization Kinetics and Processes"[28] was working on the evaluation of termination rate coefficients. It was stated that due to the strong dependency on the polymerization system (chain length, conversion, viscosity, temperature etc.); it is very difficult to compare and to obtain termination rate coefficients that could be used for all the systems. Therefore an empirical termination model of k_t in a similar manner that was done by Russell *et al.*[19] and describing the different conversion areas, was chosen but the parameters of eq. (1-4) were determined to fit our experimental conditions. The model contains four different areas defined by:

$$x(MMA) < 0.35: k_t = k_{t,0} * (1 - x(MMA)) \quad (1)$$

$$0.35 \le x(MMA) < 0.5: \ln(k_t) = 27.5 - 35 * x(MMA) \quad (2)$$

$$0.5 \le x(MMA) < 0.78: \ln(k_t) = 15 - 10 * x(MMA) \quad (3)$$

$$0.78 \le x(MMA) < 1: \ln(k_t) = 28 - 26.6 * x(MMA) \quad (4)$$

with k_{t0} equals to $1.984 \times 10^8 \times \exp(-5.89\ \mathrm{kJ/RT})\ \mathrm{L.mol^{-1}.s^{-1}}$.[29] The first section (eq. 1) corresponds to the segmental diffusion, whereas the second (eq. 2) is related to the translational diffusion. The following lower decrease in k_t was assigned to control by reaction diffusion (eq. 3 and 4).[27, 30] Such behavior has been already described[31] but using different experimental conditions. Buback[27] already fitted experimental data with an equation that take into account the viscosity change of the medium along the polymerization process. As such property was not determined in our work we choose the empirical termination model that led to similar k_t vs conversion dependences. This assumption is also supported by the fact that the initiator concentration range is chosen to have gel time between 30 min and 4 hours and thus the viscosity of the medium before the gel point is roughly similar and do not lead to drastic changes in the k_t behavior.

Figure 3 shows the termination rate coefficient vs. MMA conversion using the equations (1)-(4) described above.

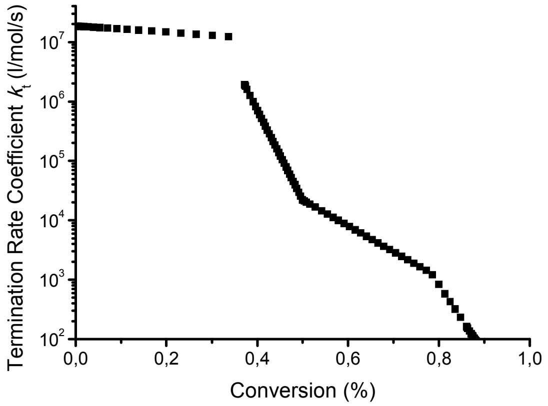

Figure 3. Empirical termination rate coefficient k_t vs. MMA conversion.

Several side reactions are first taken into account such as the transfer to monomer and initiator as well as termination by initiator radicals. As they are reactions between a macroradical and a small molecule, the free volume model, which was applied for propagation, was used for these reactions. The kinetic model is described in detail with all kinetic and physical constants in Supporting Information.

Results

Decomposition of BPO/Amine

The decomposition kinetics of BPO with a tertiary amine is crucial for the polymerization of MMA at room temperature. To our knowledge there is nevertheless no Arrhenius law which could be used to model this reaction. The mechanism is a complex reaction sequence with a nucleophilic attack of the tertiary amine on the peroxide bond of the BPO molecule followed by a redox reaction and formation of a benzoyloxy and an anilinomethyl radical that is a carbon-centered radical derived from the tertiary amine (Figure 4).[32] The decomposition of the benzoyloxy radical to CO_2 and a phenyl radical[33] was not taken into account for this model.

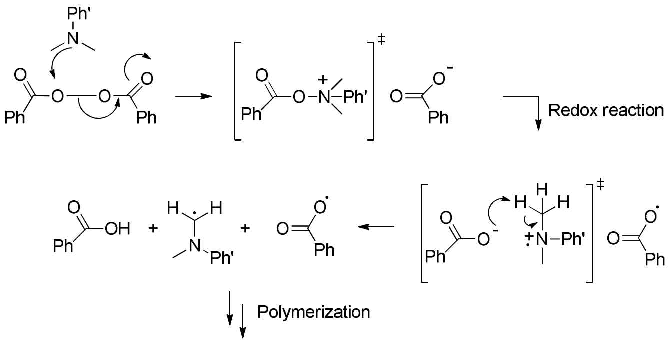

Figure 4. BPO activation and formation of radicals with tertiary amine.

Preliminary decomposition studies were unsuccessfully performed by HPLC since no good separation of the reactants could be obtained (see ESI for details). On the contrary, ^{13}C-NMR allowed a good separation of both reactants and products but to obtain a good signal to noise ratio, the concentration of the reactant has to be above 0.05 mol.L^{-1} accelerating the kinetics too much to allow its study by this technique. and this whatever the temperature (– 20 to 20 °C, see ESI for details).

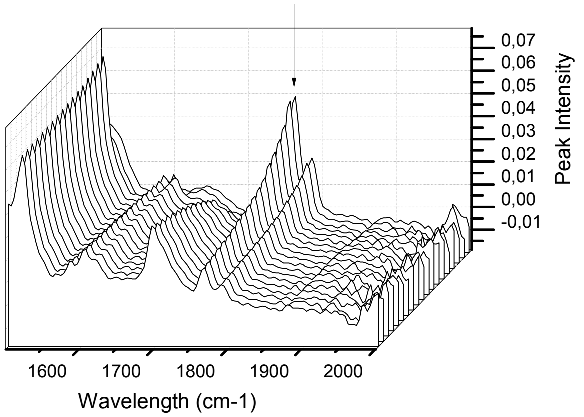

Figure 5. IR-spectra of the reaction 0.1M BPO + 0.1M DHEPT in $CHCl_3$ at 25 °C.

The kinetics was finally studied by IR in chloroform with different equimolar concentrations (0.01 M – 0.1 M) of BPO/Amine at several temperatures (0 °C – 50 °C). Below 0.01 M the noise is too important to give analyzable results and above 0.1 M, the reaction is too fast to be correctly monitored. The peroxide signal of BPO at 1760 cm^{-1} was used to follow its decomposition (Figure 5). More detailed spectra are shown in ESI.

Figure 6a shows the Arrhenius plot of the BPO/DMT and BPO/DHEPT decomposition kinetics. The following Arrhenius equations were then obtained:

$$\ln k_{\mathrm{d}}(DMT) = -26.0\ kJ/RT + \ln 832 \tag{5}$$

$$\ln k_{\mathrm{d}}(DHEPT) = -33.4\ kJ/RT + \ln 7400$$

The half-life of BPO 0.1 M using an equimolar ratio is close to 10 min at 20 °C. Such a fast initiation kinetics is totally different from the one observed in the case of the bulk polymerization of MMA initiated by AIBN between 50 and 80 °C where a constant amount of initiating radicals is produced. In our conditions, more than half of the initiating species are consumed before the onset of the polymerization, that means before the net increase of the temperature or beginning of the gel point (Figure 6b). This result showed that the majority of the polymerization takes place with little or no initiation by the BPO/Amine system. This feature is characteristic of the polymerization of methacrylate derivatives since in similar conditions the bulk styrene polymerization do not lead to complete conversion (data not shown). The trapped PMMA macroradicals were already reported to be long-lived and then able to propagate for hours. [34]

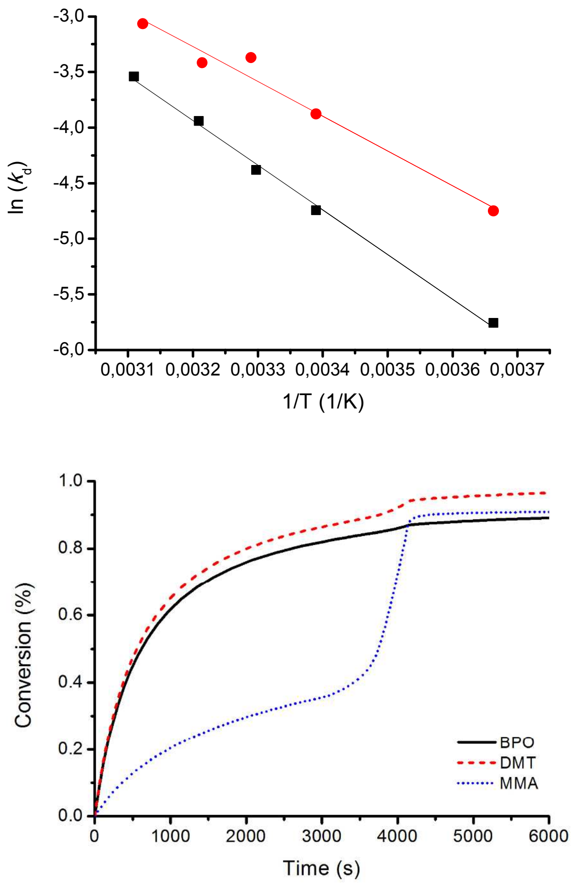

Figure 6. a) Arrhenius plot of the decomposition of BPO + DMT (red dots) / DHEPT (black squares). b) Conversion vs time plot of the bulk MMA polymerization initiated by 0.75 mol% BPO + 0.75 mol% DMT.

Analogy between reaction temperature and conversion

The bulk polymerization of MMA initiated at room temperature using the bi-component initiating system BPO/DMT was experimentally analyzed by following the increase of the temperature. A classical experiment is represented in Figure 7. The polymerization proceeds smoothly during the first 30 min and then the medium becomes suddenly very viscous and finally glassy with a lot of difficulties to determine the conversions. Nevertheless to compare the experimental data to the PREDICI simulations, the conversion accordance with temperature curves was checked by ^{1}H NMR on a reference experiment (Figure 7). The conversion at the on-set of the temperature curve was measured to 40 %, which corresponds also to the region of the beginning of the gelation.[25] The maximum of temperature was observed at 80% conversion. The end of the polymerization was considered to be when the temperature cooled down and was measured at 90 % of conversion. These experimental and characteristic temperature data will be compared in the following study to the conversion profile given by the PREDICI simulations.

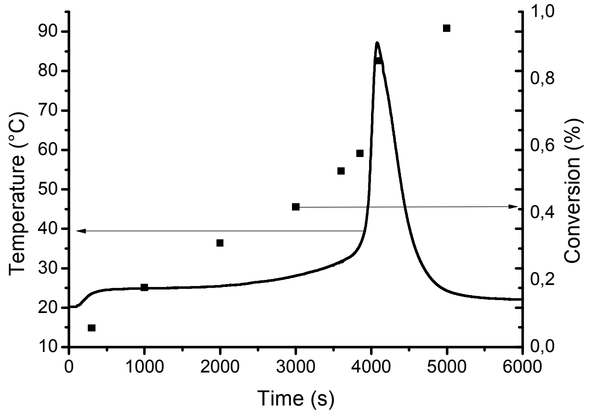

Figure 7. MMA conversion (square) compared to temperature (line) during polymerization.

Investigation on the importance of side reactions

Several side reactions (transfer to monomer/initiator and termination by initiator) are usually taken into account in the different models that were developed for the radical polymerization of methacrylate derivatives in bulk. It is important to know however which reactions steps are important in our conditions to obtain a robust model without too many estimated or known in the literature widespread constants (transfer constant to monomer for example[35]). The polymerization was first modeled with all reactions as a reference result. The conversion and SEC data for the model without transfer to monomer C_{M} and without termination by initiator radicals does not show significant difference. These parameters were consequently discarded from the model (see ESI for details). In contrary, the transfer-to-initiator, especially to the amine, reaction plays an important role as seen in Figure 8. The conversion vs. time plot stays rather similar, but it can be observed that the experimental bimodal distribution that is also observed in the simulations by considering all the constants becomes a distribution with almost two separated species if the transfer-to-amine reaction is discarded.

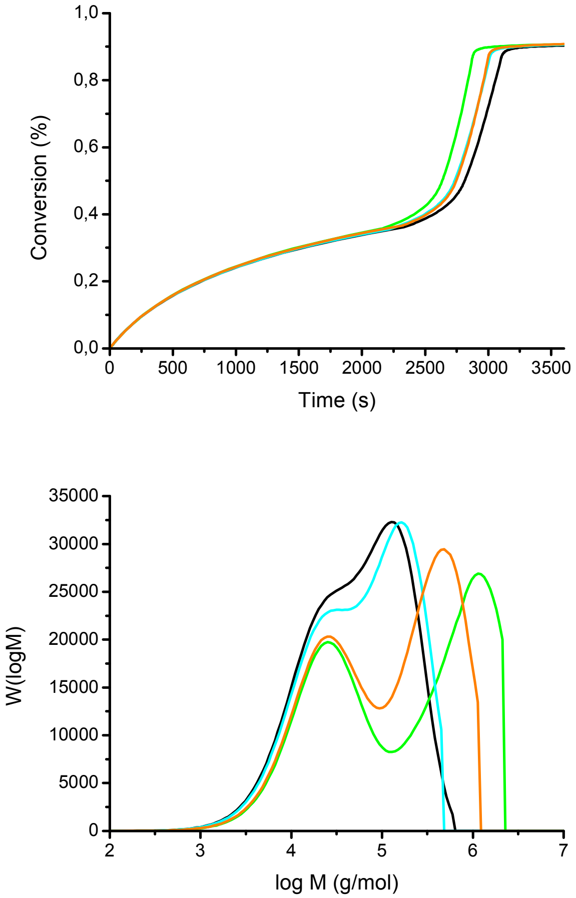

Figure 8. a) Conversion rate vs. time with all reaction steps (black line), without transfer to both BPO and DMT (green line), without transfer to BPO (blue line) and without transfer to DMT (orange line). b) SEC data with all reaction steps (black line), without transfer to both BPO and DMT (green line), without transfer to BPO (blue line) and without transfer to DMT (orange line).

Bimodal Molecular Weight Distribution (MWD)

The bimodal molecular weight distribution (MWD) of MMA bulk polymerization has already been described at high temperature (above 50 °C).[20] It takes place during the gelation when the conversion is increasing almost instantly and the termination rate drops rapidly. This phenomenon was only roughly modeled in some publications[15] since the conversion time dependence was the main parameter studied in diffusion-controlled polymerization of methacrylate derivatives.[36, 37] In our experimental conditions, bimodal distributions can be observed in both experimental SEC results and modeled data (Figure 9). The experimental and modeled MWD are in rather good agreement with only experimentally a less pronounced population of high molecular weight for high initiator concentration (see ESI for details).

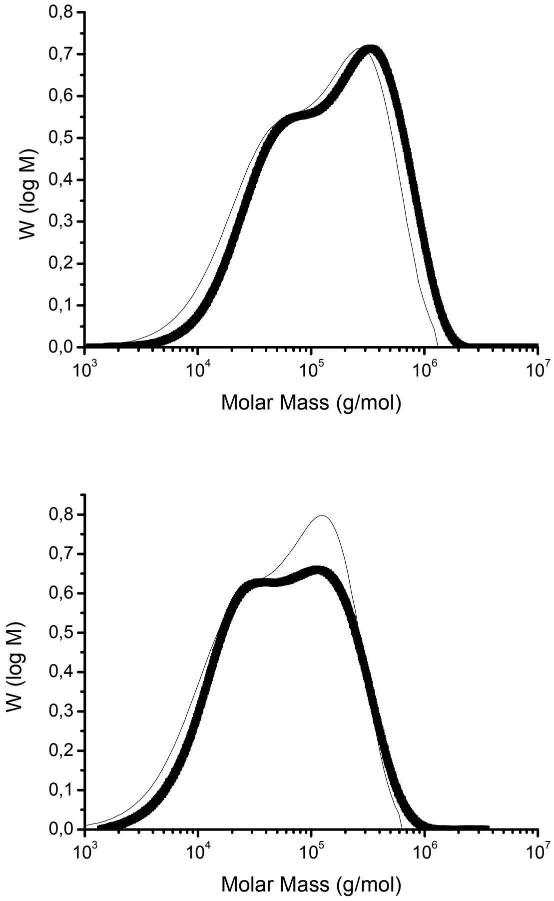

Figure 9: Modeled (thin line) and measured SEC data (thick line) from MMA polymerization with a) 0.5 mol% BPO + 0.5 mol% DMT. b) 1 mol% BPO + 1 mol% DMT.

The simulation allowed us to investigate the mechanism of the polymerization by following the change of the MWD during the polymerization process. As seen in Figure 10, a first population of low molecular weight is created at the beginning of the reaction. The molecular weight of this first population is dependent on the initiator concentration (see ESI) and this value does not change much before the gel point even if the most of the initiating system has been consumed (Figure 10). Once the gel point is reached, a second population of high molecular weight grows up. This second population comes from the rapid growth of the macroradical species that cannot self-terminate (because of the too high viscosity of the media). Such phenomenon is characteristic of the RT polymerization of methacrylate derivatives even if a small shoulder of higher molecular weight at high conversion had also been described by Zetterlund et al.[38] for the styrene polymerization at 70 °C. The presence of such living PMMA macroradicals at the gel point and in the final materials was proved by ESR analyses that were carried out during the curing of bone cement.[34]

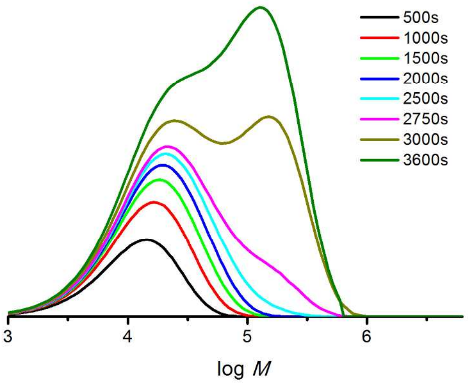

Figure 10. Modeled SEC data (thick line) from MMA polymerization initiated with 0.5 mol% BPO + 0.5 mol% DMT.

MMA polymerization with BPO/DMT

The polymerization of MMA initiated by the bi-component system BPO/DMT was studied with different equimolar initiator concentrations (from 0.25 mol% to 1.5 mol%). The results are gathered in Table 1. The influence of the initiator concentration on the polymerization kinetics is shown in Figure 11. As expected, the polymerization time decreases when increasing the initiator concentration. The polymerization takes only 35 min with a BPO and DMT concentration of 1.5 mol% and 185 minutes for an initiating system at 0.25 mol%.

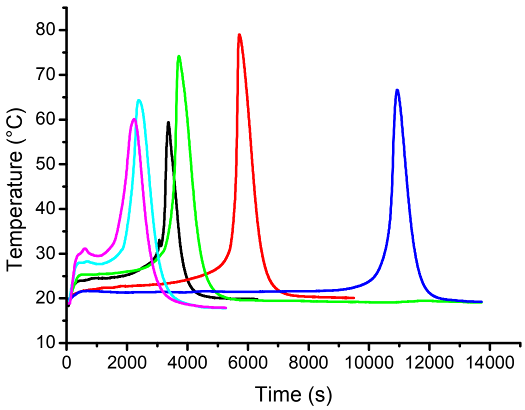

Figure 11. Temperature curves vs. time for different initiator concentrations of BPO/DMT (1.5 mol% pink, 1.25 mol% light blue, 1 mol% black, 0.75 mol% green, 0.5 mol% red, 0.25 mol% blue).

It has to be noticed that an increase of temperature is observed at the beginning of the reaction when increasing the initiator concentration probably due to the exothermic decomposition reaction between the peroxide and the tertiary amine. For lower initiator concentrations the energy coming from the initiator decomposition is directly evacuated by the reaction environment. The typical temperature profile of the polymerization and the conversion simulated with PREDICI is shown in Figure 12. Typically, the time corresponding to the maximum temperature (the gel point) should be between the times corresponding to 40 and 80 % conversion as given by the PREDICI simulations. In order to obtain better matching between experimental and theoretical data, only the initial efficiency and the transfer coefficient from macroradical to tertiary amine were fitted to 0.2 and 0.3 respectively. These both values were chosen since the decrease of efficiency with temperature is well documented[39] and for example, a value of 0.18 for the UV decomposition of azo derivatives at 10 °C has been reported.[40] Recently Matyjaszewski[41] and coworkers estimated the transfer coefficient between polyacrylate macroradicals and tertiary amines to 0.2, that is a similar order of magnitude as our estimate.

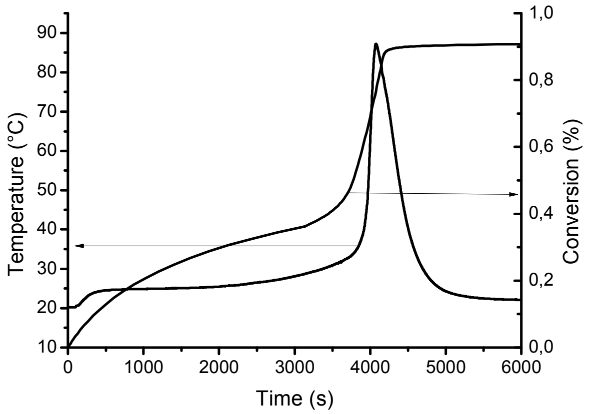

Figure 12. Temperature profile vs. modeled conversion for 0.75 mol% BPO/DMT.

Whatever the initiator concentration (Table 1), the experimental and simulated values of both the polymerization time and the molar mass distribution (M_n and M_w) are in rather good agreement. It is here important to note that since the model is used in very large conditions (0.25 mol% - 1.5 mol% initiator concentration, different initiators, different PMMA/MMA ratio), it was unrealistic to expect a total and perfect agreement between the theoretical and experimental data.

MMA polymerization with BPO/DHEPT

The model, that was developed for the BPO/DMT initiation system was used as well for the BPO/DHEPT system. DHEPT was investigated in this study as it has already been used in commercial adhesive systems.[42, 43] For biomedical applications for example, DHEPT is chosen because of its lower toxicity compared to DMT. The temperature profiles of the polymerization reactions with different initiator concentrations are similar to those of BPO/DMT. The more initiator is used, the faster is the polymerization time. Polymerizations are interestingly faster compared to BPO/DMT (40 min for 1.5 mol% DHEPT and one hour for DMT), although the decomposition rate of BPO/DHEPT is lower than that of BPO/DMT at room temperature (Figure 6). This should normally lead to a decrease of the rate of polymerization, which is not observed experimentally.

To fit the PREDICI simulations and the experimental data, adjustments of some of the amine-specific parameters (efficiency $f_{\text{BPO/DHEPT}}$, and the transfer constant to amine C_{DHEPT}) were necessary. The accordance between simulated and experimental data is gathered in Table 2. The time of the peak temperature is with these adjustments in the range of the model data obtained by PREDICI.

The higher rate of polymerization for the BPO/DHEPT system led us to change the overall efficiency of the radical production since in the same time the M_n and M_w of the first population of polymer chains are also lower than in case of DMT and thus more radicals should be produced. Using an initial efficiency of 0.3 instead of 0.2 allowed a better fit of the experimental kinetic data. The increase of efficiency may be explained by a slightly lower bond dissociation energy (BDE) of the C-H bond when the methyl group of the DMT is substituted by an hydroxy ethyl group. This has already been reported by Lalevee and coworkers[44] on the reactivity of triethylamine and methyldiethanolamine (91.2 and 87.1 kcal.mol^{-1} respectively). The fit of the MWD requires also adjustments of the transfer constant to amine C_{DHEPT} with a value of 0.15 instead of 0.3 for DMT.

Such lower value is not in agreement with the lowering of BDE. This lower C_{DHEPT} may be explained by the presence of four instead of six labile hydrogens on the amino compounds coupled with a higher steric hindrance brought by the presence of two hydroxy ethyl groups. DFT calculations and a detailed kinetic study in the presence of excess amine are necessary to confirm these assumptions.

PMMA/MMA syrup polymerization with BPO/DHEPT

A mixture of PMMA and MMA with ratios between 25/75 and 15/85 was studied and modeled. These syrups enable faster polymerization times and higher viscosities before polymerization. The practical handling of these syrups is often easier when applied technically, e.g. in dentistry or construction.

The same model as above was applied with 75 % - 85 % of MMA and 25 % - 15 % of PMMA in the starting mixture. The initiator concentration is based on the sole concentration of MMA. The experimental MWD of the polymer is inserted in the PREDICI simulations as starting materials.

Experimentally, the temperature peaks are broadened compared to pure MMA polymerization, what might be due to the polymer chains, which have a lower heat capacity than MMA and the higher viscosity of the medium, that led to a less efficient evacuation of the calories (Figure 12a).

The simulated kinetics profiles for the three syrups with 75/25, 80/20 and 85/15 PMMA/MMA ratios, are in good agreement with the experimental data (see ESI for details). At low initiator concentration, the simulated polymerization is slightly faster (see ESI). The simulated SEC chromatograms are in good agreement with the experimental one (Figure 12b) even if the M_w are always underestimated. The small discrepancy between experimental and simulated MWD values might be due to some variation in the estimation of the k_t value when some polymer chains are already present in the medium.

Table 1: Comparison of experimental and simulated polymerization time and molar mass distribution values with the BPO/DMT initiating system

Initiator Concentration mol %	$t_{T,\max}$ of Polymerization s	PREDICI On-Set time s	PREDICI End of Polymerization s	M_n - SEC g/mol	M_w - SEC g/mol	M_n - PREDICI g/mol	M_w - PREDICI g/mol
0.25	9928	10500	12000	126300	535900	84400	364000
0.5	5810	5200	6100	41100	149000	42400	190000
0.75	3903	3500	4000	39700	150700	28300	127200
1	2920	2500	2900	24500	86200	21000	89700
1.25	2167	2000	2300	23600	85600	16900	76000
1.5	2063	1700	2000	16800	67500	13900	60100

Table 2: Comparison of experimental and simulated polymerization time and molar mass distribution values with the BPO/DHEPT initiating system

Initiator Concentration mol %	$t_{T,\max}$ of Polymerization s	PREDICI On-Set time s	PREDICI End of Polymerization s	M_n - SEC g/mol	M_w - SEC g/mol	M_n - PREDICI g/mol	M_w - PREDICI g/mol
0.25	6437	7100	8100	54900	163000	69900	227000
0.5	4092	3700	4200	34200	97100	35600	120000
0.75	2625	2400	2700	25500	88500	23800	79500
1	2283	1900	2200	20800	72600	17900	61300
1.25	2133	1500	1700	16500	59400	14200	46700
1.5	2227	1300	1500	13600	49200	11900	40800

Conclusion

This study presents the development of a kinetic mathematical model for the radical bulk polymerization of MMA at room temperature. The simulations were based on physical parameters by using the free-volume theory (reactions between macromolecules and small molecules) and also an empirical model for the termination rate constant. Compared to other studies, only a couple of parameters have been estimated. The decomposition kinetics for the BPO/tertiary amine initiating system has been measured by IR and an Arrhenius plot was established and used in the model. Unlike other studies in diffusion-controlled polymerization, the initiation step is very fast and most of the initiator is consumed before the gelation point.

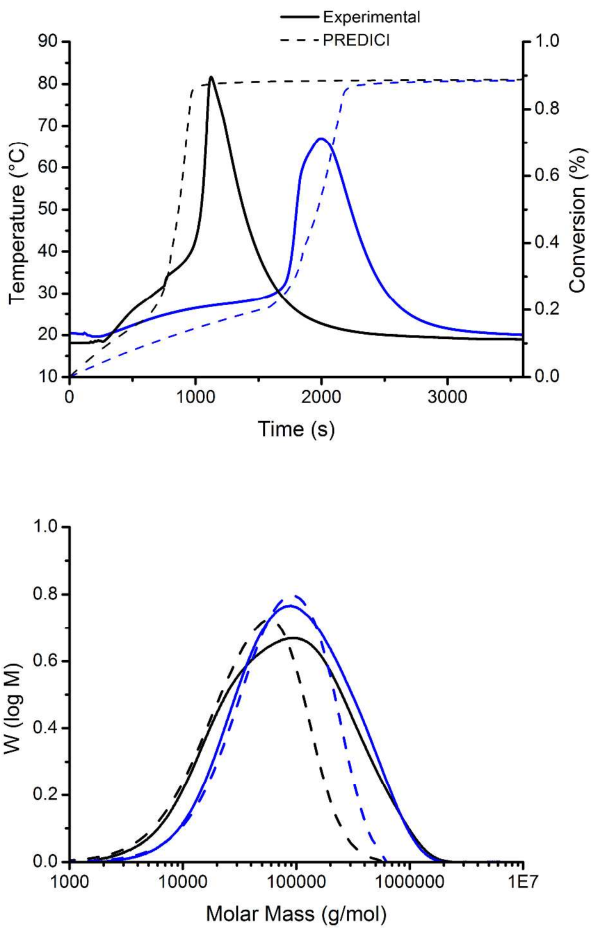

Figure 12. a) Temperature profile vs. modeled conversion for 1 (blue) and 0.5 (black) mol% BPO/DHEPT. b) Modeled (dashed line) and measured SEC data (thick line) for MMA polymerization with 1 (blue) and 0.5 (black) mol% BPO/DHEPT.

The model was successfully tested for a wide range of experimental conditions (large range of initiator concentration, different initiating systems, pure MMA bulk polymerization, and polymerization of PMMA/MMA syrups in various compositions).

Acknowledgements

The authors thank Dr. Virginie Heran (ISM2 – Aix-Marseille-University) for the help with the IR measurements.

Notes and references

Aix-Marseille Université, CNRS, Institut de Chimie Radicalaire, UMR 7273, F-13397 Marseille, France.

Electronic Supplementary Information (ESI) available: [Further information on the experimental section and a detailed model development in the supporting information]. See DOI: 10.1039/b000000x/

1. T. Buergel, R. Hettich and A. Pfeil, **2007**, Two-Component Mortal Composition and its Use,US 7,238,749.
2. B. Vazquez, J. San Roman, S. Deb and W. Bonfield, *Journal of biomedical materials research*, 1998, **43**, 131-139.
3. D. S. Zhao, N. Moritz, P. Laurila, R. Mattila, L. V. J. Lassila, N. Strandberg, T. Mäntylä, P. K. Vallittu and H. T. Aro, *Medical engineering & physics*, 2009, **31**, 461-469.
4. B. Vazquez, S. Deb and W. Bonfield, *Journal of materials science. Materials in medicine*, 1997, **8**, 455-460.
5. E. W. Fritsch, *Journal of biomedical materials research*, 1996, **31**, 451-456.
6. P. K. Vallittu, I. E. Ruyter and S. Buykuilmaz, *European Journal of Oral Sciences*, 1998, **106**, 588-593.
7. P. K. Vallittu and H. Kurunmäki, *Journal of oral rehabilitation*, 2003, **30**, 887-892.
8. R. Arino and A. Boldizar, *Polymer Engineering and Science*, 2012, **52**, 1951-1957.
9. G. M. Brauer, D. M. Dulik, J. M. Antonucci, D. J. Termini and H. Argentar, *Journal of dental research*, 1979, **58**, 1994-2000.
10. I. D. Sideridou, D. S. Achilias and N. C. Kostidou, *Journal of Applied Polymer Science*, 2008, **109**, 515-524.
11. S. Leonard-Williams, *Reinforced Plastics*, 2008, **52**, 28-29.
12. L. Horner and K. Scherf, *Justus Liebigs Annalen der Chemie*, 1951, **573**, 35-55.
13. J. Lal and R. Green, *Journal of Polymer Science*, 1955, **17**, 403-409.
14. D. K. Garg, C. Serra, Y. Hoarau, D. Parida, M. Bouquey and R. Muller, *Macromolecules*, 2014, **47**, 4567-4586.
15. G. D. Verros, T. Latsos and D. S. Achilias, *Polymer*, 2005, 539-552.
16. D. S. Achilias, *Macromolecular Theory and Simulations*, 2007, **16**, 319-347.
17. D. S. Achilias and I. D. Sideridou, *Macromolecules*, 2004, **37**, 4254-4265.
18. M. Wulkow, *Macromolecular Reaction Engineering*, 2008, **2**, 461-494.
19. G. T. Russell and D. H. Napper, *Macromolecules*, 1988, **21**, 2133-2140.
20. S. T. Balke and A. E. Hamielec, *Journal of Applied Polymer Science*, 1973, **17**, 905-949.
21. C. H. Bamford, G. C. Eastmond and D. Whittle, *Polymer*, 1969, **10**, 771-783.
22. M. D. Zammit, T. P. Davis, D. M. Haddleton and K. G. Suddaby, *Macromolecules*, 1997, **30**, 1915-1920.
23. M. M. Alghamdi and G. T. Russell, *Macromolecular Chemistry and Physics*, 2013, **214**, 1384-1395.

24. D. S. Achilias and C. Kipasissides, *Macromolecules*, 1992, **25**, 3739-3750.
25. M. v. Smoluchowski, *Zeitschrift für physikalische Chemie*, 1916, **XCII**, 129-168.
26. O. J. Karlsson, J. M. Stubbs, L. E. Karlsson and D. C. Sundberg, *Polymer*, 2001, **42**, 4915-4923.
27. M. Buback, *Makromolekulare Chemie*, 1990, **191**, 1575-1587.
28. M. Buback, M. Egorov, R. G. Gilbert, V. Kaminsky, O. F. Olaj, G. T. Russell, P. Vana and G. Zifferer, *Macromolecular Chemistry and Physics*, 2002, **203**, 2570-2582.
29. D. R. Taylor, K. Y. van Berkel, M. M. Alghamdi and G. T. Russell, *Macromolecular Chemistry and Physics*, 2010, **211**, 563-579.
30. S. Beuermann and M. Buback, *Prog. Polym. Sci.*, 2002, **27**, 191-254.
31. M. Buback and C. Kowollik, *Macromolecules*, 1999, **32**, 1445.
32. X.-D. Feng, *Makromolekulare Chemie. Macromolecular Symposia*, 1992, **63**, 1-18.
33. M. Buback, H. Frauendorf, F. Gunzler and P. Vana, *Polymer*, 2007, **48**, 5590-5598.
34. F. F. Oldfield and H. K. Yasuda, *Journal of Biomedical Materials Research*, 1999, **44**, 436-445.
35. J. Brandrup, E. H. Immergut and E. A. Grulke, *Polymer Handbook*, 4 Edition edn., Wiley-Interscience, 2003.
36. M. Stickler, D. Panke and A. E. Hamielec, *Journal of Polymer Science*, 1984, **22**, 2243-2253.
37. J. N. Cardenas and K. F. O'Driscoll, *Journal of Polymer Science: Polymer Chemistry Edition*, 1976, **14**, 883-897.
38. P. B. Zetterlund, H. Yamazoe and B. Yamada, *Macromolecular Theory and Simulations*, 2003, **12**, 379-385.
39. G. Moad and D. Solomon, *The Chemistry of Radical Polymerization 2nd fully revised edition*, Elsevier, 2002.
40. Y. Guillaneuf, J.-L. Couturier, D. Gigmes, S. R. A. Marque, P. Tordo and D. Bertin, *Journal of Organic Chemistry*, 2008, **73**, 4728-4731.
41. T. G. Ribelli, D. Konkolewicz, S. Bernhard and K. Matyjaszewski, *Journal of the American Chemical Society*, 2014, **136**, 13303-13312.
42. K. L. Van Landuyt, J. Snauwaert, J. De Munck, M. Peumans, Y. Yoshida, A. Poitevin, E. Coutinho, K. Suzuki, P. Lambrechts and B. Van Meerbeek, *Biomaterials*, 2007, **28**, 3757-3785.
43. N. Karim, J. D. Oxman, A. S. Abuelyaman and B. N. Gaddam, **2005**, Dental Materials with extendable work time, kits, and methods,US 6,964,985.
44. J. Lalevée, X. Allonas and J. P. Fouassier, *Journal of the American Chemical Society*, 2002, **124**, 9613-9621.

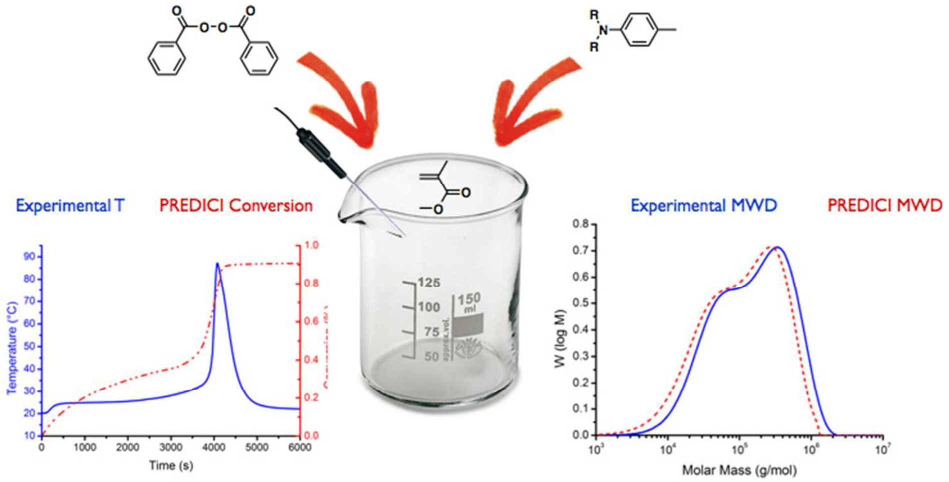

77x40mm (254 x 254 DPI)